Interleaved LLC (iLLC) Resonant Converter with Hybrid Rectifier and Variable-Frequency Plus Phase-Shift (VFPPS) Control For Wide Output Voltage Range Applications

Hongfei Wu, *Member*, *IEEE*, Xiaohai Zhan, Yan Xing, *Member, IEEE*

Abstract— **A family of two-phase interleaved LLC (iLLC) resonant converter with hybrid rectifier is proposed for wide output voltage range applications. The primary sides of the two LLC converters are in parallel, and the connection of the secondary windings in the two LLC converters can be regulated by the hybrid rectifier according to the output voltage. Variable frequency control is employed to regulate the output voltage and the secondary windings are in series when the output voltage is high. Fixed-frequency phase-shift control is adopted to regulate the configuration of the secondary windings as well as the output voltage when the output voltage is low. The output voltage range is extended by adaptively changing the configuration of the hybrid rectifier, which results in reduced switching frequency range, circulating current and conduction losses of the LLC resonant tank. Zero voltage switching and zero current switching are achieved for all the active switches and diodes, respectively, within the entire operation range. The operation principles are analyzed and a 3.5kW prototype with 400V input voltage and 150V-500V output voltage is built and tested to evaluate the feasibility of the proposed method.**

Index Terms—**LLC resonant converter, wide voltage range, rectifier, variable configuration, phase-shift control**

I. INTRODUCTION

LLC resonant converter is one of the most attractive topologies for its features of excellent soft-switching performance and high power density. It has been applied in several applications such as server farms [1], LED drivers [2], battery chargers [3], electric vehicle [4] and renewable power systems [5] etc. Although extensive researches on design, modeling and control of LLC resonant converters have been carried out by academia and industry departments, LLC resonant converters are still evolving [6][7]. Tradeoff between conversion efficiency and operation range is still necessary to meet the needs of various applications. As a result, new topological variations and innovations have been continuously emerging.

It has been recognized that soft-switching performance, high power density and high efficiency are the most attractive features of LLC resonant converters. It also came to recognize that LLC resonant converters have some drawbacks. For example, zero current switching (ZCS) will be lost for the rectifying diodes if the switching frequency f_s is higher than the resonant frequency f_r of the resonant tank. In addition to the loss of ZCS, it is difficult to regulate the output voltage of a LLC resonant converter in the $f_s > f_r$ region. Because the voltage-gain curve in the $f_s > f_r$ region is very flat, especially in light load condition. Therefore, LLC resonant converters are always designed to operate in the $f_s \leq f_r$ region, where zero voltage switching (ZVS), ZCS and good regulation of output voltage can be achieved easily [8]. However, it is still very difficult to realize a wide range of voltage/load regulation while maintaining high efficiency within the entire voltage and load ranges when $f_s \leq f_r$ [9]. It is because the increased circulating current of the resonant tank will hurt the conversion efficiency greatly once the operating frequency is far away from the resonant frequency. As a result, how to achieve high-efficiency in a wide voltage range by a LLC resonant converter has been an emergent research topic, especially for the applications of renewable energy and battery chargers for electric vehicles.

To improve the LLC resonant converter's operational voltage range as well as conversion efficiency within the entire operation range, quite a few methods have been proposed. Optimal design methods were proposed to extend the operational voltage range and make full use of the voltage regulation and power conversion capabilities of LLC resonant converters [10]-[12]. However, the contradiction between efficiency and voltage range is still inevitable. Burst mode control is employed to improve the conversion efficiency at low output voltage and light load conditions [13]-[15]. It is straightforward and effective, but the implementation is complicated. Meanwhile, low frequency current and voltage ripples will be introduced by the burst mode operation. Primary-side and secondary-side phase-shift control were proposed to provide another effective control freedom, so as to reduce the switching frequency range of the LLC resonant converter [16][17]. Although the conduction losses associated with the circulating current of the magnetizing inductance are reduced, the turn-off losses of switches are increased because

of the high turn-off current. Another straightforward and effective method to solve the wide voltage range problem is to use variable-structure topologies. Quite a few methods have been proposed to change the circuit topology of a LLC resonant converter according to the input and output voltages. Variable structure LLC resonant converter can be achieved by changing the topology of the primary side switching network [18], regulating the equivalent turns ratio of the transformer [19], and varying the circuit of the secondary side rectifier [20]. However, the primary-side variable-structure topologies proposed in [18] and [19] are unsuitable for the wide output voltage range with constant input voltage applications, e.g. the battery charger for electric vehicles. It is because the core and conduction losses associated with the flux and the magnetizing current of the transformer increase when the output voltage increases. The secondary-side variable-structure rectifier proposed in [20] is a good candidate for wide output voltage range LLC resonant converter, but this rectifier is only valid for voltage-doubler rectifier and cannot be extended to other types of rectifier. Meanwhile, two active switches have to be used on the secondary-side, results in complicated control and driving of the circuit. Another secondary-side variable-structure topology is proposed for PWM full-bridge converter by changing the connection of multiple rectifiers [21], but this method is not valid for resonant converter because smooth mode transition is very difficult to achieve and additional conduction losses will be introduced by the auxiliary switch and diode on the secondary side. In [22]-[25], novel voltage regulation method with transformer winding series-parallel auto-regulated principles is proposed for PWM forward and full-bridge converters. This method is a good candidate for PWM converters with wide output voltage range applications. However, the conversion efficiency of these PWM converters is still slight lower than resonant converters, because the rectifying diodes are hard-switched and have to sustain a high voltage stress induced by the leakage inductance of the transformer.

The major contribution of this paper is to propose a novel voltage regulation method for LLC resonant converters through innovative hybrid rectifier and control method. A family of novel interleaved LLC (iLLC) resonant converters is harvested for wide output voltage applications. With the proposed topologies and control, the LLC resonant converters always operate in the $f_s \leq f_r$ region and the switching frequency range can be narrowed significantly. This paper is organized as follows. In section II, the basic idea used to derive iLLC resonant converters with hybrid rectifier is proposed. Operation principles of a full-bridge iLLC resonant converter with hybrid full-bridge rectifier are analyzed in section III. Characteristics of the proposed iLLC resonant converter are presented in section IV. Experimental results are presented in section IV. Finally, conclusions will be given in section VI.

II. PROPOSED ILLC RESONANT CONVERTER WITH HYBRID RECTIFIER

The structure of the proposed interleaved LLC (iLLC) resonant converter with a hybrid rectifier is shown in Fig. 1, where two LLC resonant switching networks are employed
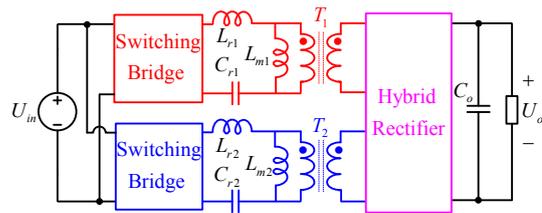

Fig. 1. Structure of the proposed interleaved LLC resonant converter with a hybrid rectifier.
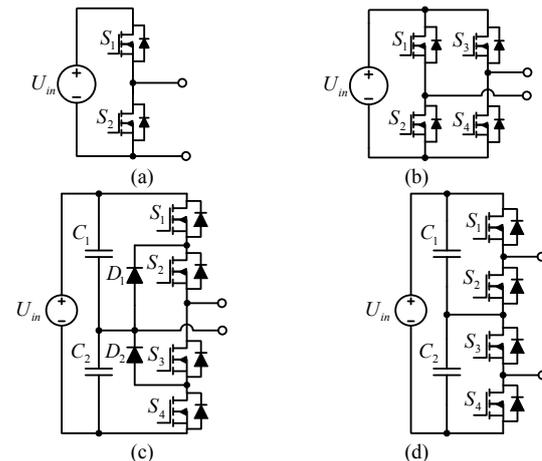

Fig. 2. Topology of the primary-side switching bridge, (a) half-bridge, (b) full-bridge, (c) and (d) three-level.
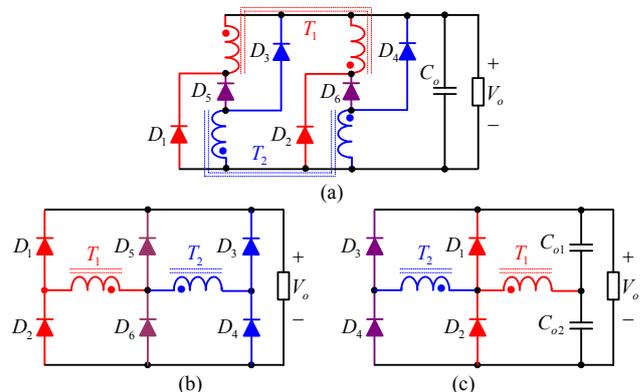

Fig. 3. Topology of hybrid rectifier, (a) center-tapped, (b) full-bridge, (c) voltage-doubler.

on the primary side and a hybrid rectifier is adopted on the secondary side. The two LLC resonant switching networks are connected in parallel, while the hybrid rectifier on the secondary side is shared by the two secondary windings of the two transformers, T_1 and T_2. The LLC resonant switching network on the primary side is composed a switching-bridge and a LLC resonant network. As illustrated in Fig. 2, the switching-bridge can be a half-bridge, full-bridge or three-level-bridge.

The topology of the hybrid rectifier in the proposed iLLC resonant converter is shown in Fig. 3, where it is seen that the hybrid rectifier can be center-tapped type, full-bridge type and voltage-doubler type. Generally speaking, the center-tapped rectifier is suitable for applications with low output voltage and high output current, while the
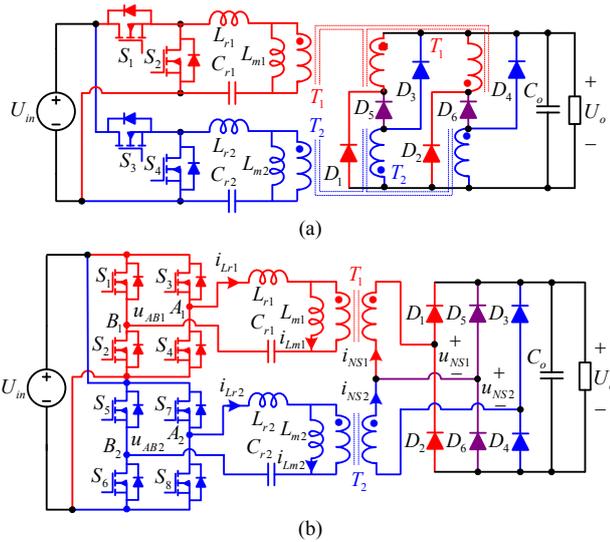
Fig. 4. Examples of interleaved LLC resonant converter with hybrid rectifier, (a) half-bridge, (b) full-bridge.

voltage-doubler rectifier is suitable for applications with high output voltage. The two secondary windings in the proposed iLLC resonant converter can be connected in-series or not through the hybrid rectifier. The operation of the hybrid rectifier and connection of the two secondary windings are regulated by the phase-shift angle between the two LLC resonant switching networks on the primary side. Therefore, a new control freedom is provided by the iLLC and the hybrid rectifier. As a result, the output voltage can be regulated in a wide range without varying the switching frequency of the iLLC resonant converter.

A family of novel iLLC resonant converters can be harvested by replacing the block diagrams in Fig. 1 with corresponding circuits shown in Fig. 2 and Fig. 3, respectively. Two examples of iLLC resonant converter topology are shown in Fig. 4, where Fig. 4(a) is a half-bridge iLLC resonant converter with center-tapped hybrid rectifier while Fig. 4(b) is a full-bridge iLLC resonant converter with a full-bridge hybrid rectifier.

III. ANALYSIS ON THE PROPOSED FULL-BRIDGE ILLC RESONANT CONVERTER

In this section, the full-bridge iLLC resonant converter shown in Fig. 4(b) is taken as an example to be analyzed to verify the operation principles and feasibility of the proposed method. Variable-frequency plus phase-shift (VFPPS) control is employed to the proposed iLLC resonant converter to regulate the output voltage in a wide output voltage range. Variable frequency control is adopted to regulate the output voltage and the secondary windings are in series when the output voltage is high. Fixed-frequency phase-shift control is adopted to regulate the output voltage by adaptively changing the connection of the two secondary windings when the output voltage is low. To simplify the analysis, the normalized voltage gain, G_i, is defined as:
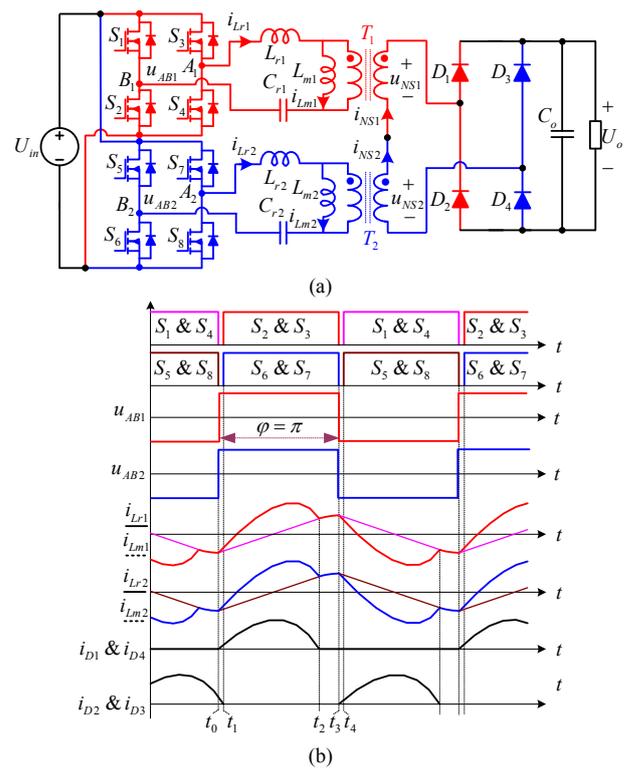
$$G_i = \frac{U_o}{N U_{in}} \tag{1}$$

Fig. 5 Equivalent circuit and key waveforms in the variable-frequency mode, (a) equivalent circuit, (b) key waveforms.

where U_o and U_{in} are the output and input voltage, respectively, while N is the secondary to primary turns ratio of the transformers T_1 and T_2. The phase shift angle φ is defined to be the phase difference between the gate signals of switch pairs $S_2\&S_3$ and $S_5\&S_8$. The control of the converter is achieved by varying the switching frequency f_S or the phase shift angle φ.

A. Variable-Frequency Mode

When the iLLC converter operates in the variable-frequency mode, the switching frequency f_S is employed to regulate the output. f_S is lower than the resonant frequency, f_r, of the resonant tank and the phase shift angle φ is kept at its maximum value, i.e. $\varphi=\pi$. Therefore, all the switches S_1-S_8 have the constant duty cycle of 0.5, the switches S_1, S_4, S_5 and S_8 are gated on/off simultaneously, while S_2, S_3, S_6 and S_7 are on/off simultaneously. In this mode, the voltages, u_{AB1} and u_{AB2}, produced by the switching bridges of the two LLC modules are always in phase. Therefore, the voltages, u_{NS1} and u_{NS2}, on the secondary-windings of the two transformers T_1 and T_2 are in phase as well. It means the two secondary windings always operate in in-series manner. As a result, the rectifying bridge composed of D_5 and D_6 and shared by the two secondary windings does not work.

The equivalent circuit and key waveforms of the proposed iLLC resonant converter in the variable-frequency mode are illustrated in Fig. 5. It can be seen that the hybrid rectifier has degraded to be a conventional full-bridge rectifier. The iLLC converter can be treated as a traditional variable-frequency modulated LLC resonant converter with split primary-side circuits and transformers. Therefore, the operation principles

and waveforms of the iLLC resonant converter are the same as the conventional LLC resonant converter. The detailed operation principles in the variable frequency mode will not be analyzed here.

It should be noted that the current flows through the resonant tanks and the transformer windings of the two LLC modules are always the same because the secondary windings are always in-series. Because of the primary-side parallel and secondary-winding series structure, the normalized voltage gain of the iLLC is two times of the normalized voltage gain G_{LLC} of each LLC module, i.e. $G_i=2G_{LLC}$.

B. Fixed-Frequency Phase-Shift Mode

If the switching frequency f_S has been increased to f_r and the output voltage continuous to decrease, the iLLC resonant converter will enter the fixed-frequency phase-shift mode, in which f_S is kept at its maximum value, i.e. $f_S=f_r$, and the phase shift angle φ is employed to regulate the output voltage. Since $\varphi<\pi$ and the voltages u_{AB1} and u_{AB2}, and voltages u_{NS1} and u_{NS2} are not in phase, the connection of the secondary windings of T_1 and T_2 will be regulated by the polarity of u_{NS1} and u_{NS2}. Since the two LLC modules operates at its resonant frequency, it is obvious that $G_i=2$ if $\varphi=\pi$ and the two secondary windings work in in-series manner, whereas $G_i=1$ if $\varphi=0$ and the two secondary windings work in in-parallel manner. Therefore, by regulating the phase shift angle φ and without increasing the switching frequency, the normalized voltage gain G_i can be regulated continuously between 1 and 2. As a result, the phase shift angle can be used as a new control freedom to regulate the output voltage in a wide range, and the output voltage range regulated by the switching frequency mode can be narrowed significantly.

The LLC module composed of S_1-S_4 is defined as the lagging-module, while the LLC module composed of S_5-S_8 is defined as the leading-module. It means the gate signals of S_5-S_8 lead the corresponding gate signals of S_1-S_4.

1) Case I: $0<\varphi<\pi$

The parameters of the two LLC modules are assumed to be the same. The key waveforms of the proposed iLLC converter with $0<\varphi<\pi$ are shown in Fig. 6. It should be noted that the operation waveforms of the converter are only determined by the phase shift angle and has nothing to do the transferred power. There are six switching stages in half switching cycle. The equivalent circuit of each switching Stage is shown in Fig. 7.

Stage I [t_0, t_1][Fig. 7(a)]: Before t_0, switch pairs $S_1\&S_4$ and $S_6\&S_7$ are ON, all the diodes on the secondary-side are OFF. At t_0, $S_1\&S_4$ are turned OFF, the body diodes of S_2 and S_3 are ON due to the negative resonant current i_{Lr1}. Meanwhile, the diodes D_1 and D_4 on the secondary side begin to conduct, because the polarities of voltages, u_{NS1} and u_{NS2}, of the two secondary windings are the same. Therefore, the secondary windings operates in-series and the currents flow through the secondary windings, i_{NS1} and i_{NS2}, are the same.

Stage II [t_1, t_2][Fig. 7(b)]: At t_1, switches S_2 and S_3 are turned-ON with zero voltage.

During Stage I and II, L_{r1} and L_{r2} resonate with C_{r1} and C_{r2}, respectively, and the currents of the two magnetizing inductors, L_{m1} and L_{m2}, increase linearly. The voltages applied
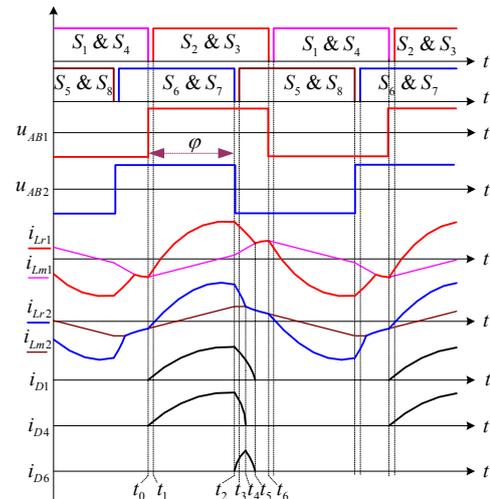

Fig. 6. Key waveforms of the iLLC converter in the phase-shift mode.

on the two secondary windings

$$u_{NS1} = u_{NS2} = \frac{U_o}{2} \qquad (2)$$

Stage III [t_2, t_3][Fig. 7(c)]: At t_2, the switches $S_6\&S_7$ are turned OFF, the body diodes of $S_5\&S_8$ are ON due to the positive current of i_{Lr2}. Then, the polarity of voltage u_{AB2} becomes negative. As a result, the diode D_6 begins to conduct due to the forward-biased voltage. According to the equivalent circuit shown in Fig. 7(c), when both D_6 and D_4 are ON, the secondary winding of T_2 is shorted and the current i_{Lr2} decreases rapidly. Hence, the two secondary windings are not in-series any more.

Stage IV [t_3, t_4][Fig. 7(d)]: At t_3, the switches $S_5\&S_8$ are turned-ON with zero-voltage.

During Stage III and Stage IV, L_{r1} and L_{r2} resonate with C_{r1} and C_{r2}, respectively, but only the transformer T_1 transfers power to the output. The voltages u_{NS1} and u_{NS2} satisfy:

$$\begin{cases} u_{NS1} = U_o \\ u_{NS2} = 0 \end{cases} \qquad (3)$$

Stage V [t_4, t_5][Fig. 7(e)]: At t_4, the current i_{NS2} decreases to zero and the diode D_4 is OFF. i_{NS2} stays in zero in this Stage because $U_o>G_{LLC}U_{in}$. Therefore, L_{r2} and L_{m2} begin to resonate with C_{r2}. D_1 and D_6 are ON and only transformer T_1 supplies power to the load in this Stage.

Stage VI [t_5, t_6][Fig. 7(f)]: At t_5, the current i_{NS1} decreases to zero, and the diodes D_1 and D_6 are OFF. L_{r1} and L_{m1} begin to resonate with C_{r1}.

According to the operation principles, it is seen that the leading-module only transfers power to the load in the Stage I and Stage II, while the lagging-module transfers power in Stage I-Stage IV. Therefore, the transferred power of the two modules in the fixed-frequency mode is not the same. More specifically, the power ratio of the leading module decreases and the power ratio of the lagging module increases when the phase-shift angle decreases. From this point of view, the proposed converter is more suitable for the applications of battery charging for electric-vehicle and energy storage system, where the charging power decreases linearly with the decreasing of the battery voltage. In this case, even though the power ratio of the lagging-module is greater than the
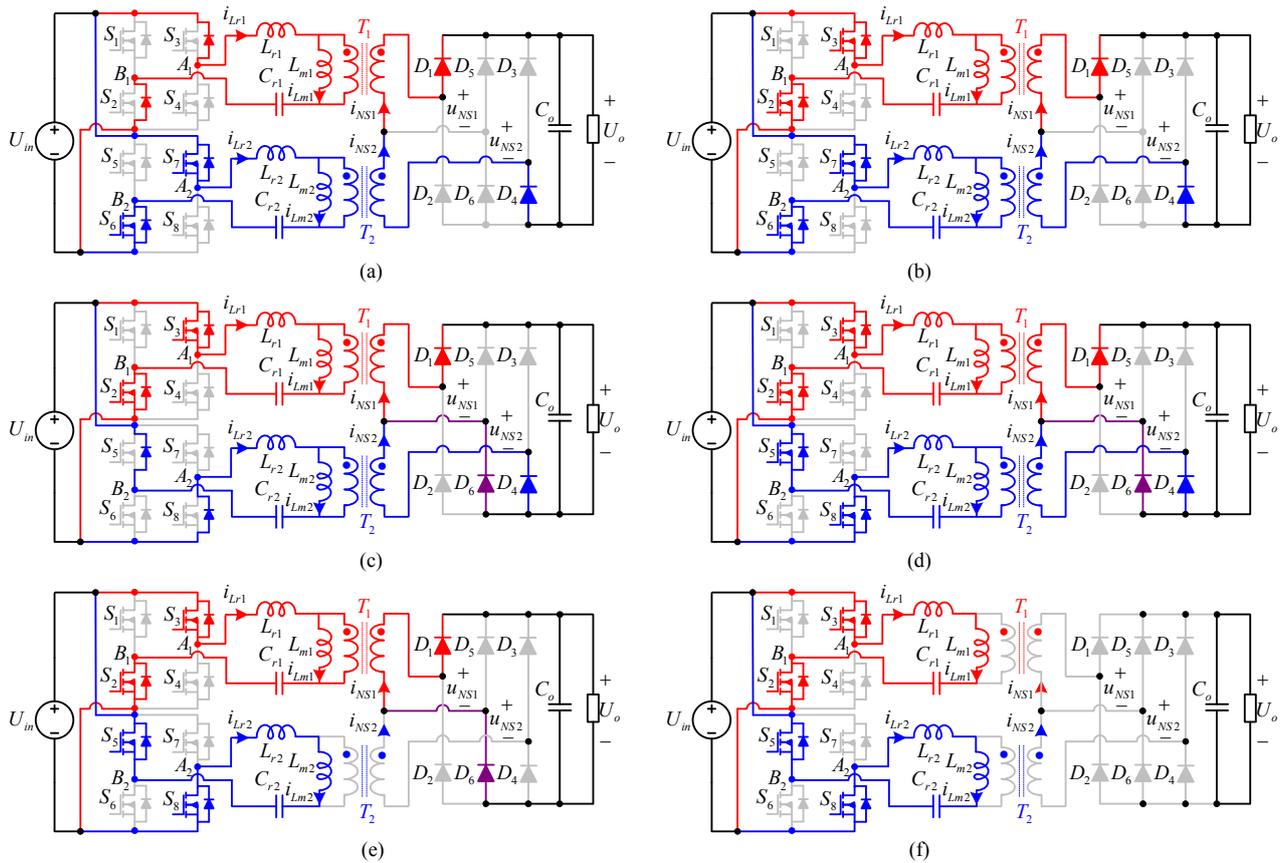
Fig. 7. Equivalent circuit of the phase-shift mode, (a) $[t_0, t_1]$, (b) $[t_1, t_2]$, (c) $[t_2, t_3]$, (d) $[t_3, t_4]$, (e) $[t_4, t_5]$, and (f) $[t_5, t_6]$.

leading-module in the fixed-frequency mode, the power rating of the lagging-module in the fixed-frequency mode is always lower than that in the variable-frequency mode, which means the power capacity of the iLLC converter is determined by the variable-frequency mode, rather than the phase-shift mode.

2) Case II: φ=0

As analyzed above, the power ratio of the leading-module in the fixed-frequency mode is proportional to the phase-shift angle φ. Therefore, when the phase shift angle approaches to zero, the output power of the leading-module will approaches to zero as well. However, the situation will be changed once φ=0, because the two modules will work in parallel when φ=0. Theoretically, the current will be shared by the two modules if the parameters of the resonant tanks, transformers, switches and diodes are all the same. However, in practice, it is very difficult to ensure the consistency of parameters. Considering that the output voltage and power is at its minimum value when φ=0, and the fact that the output power of the leading-module will approaches to zero when the phase shift angle approaches to zero, one can shut down the leading-module to avoid the current-sharing issue in the case of φ=0. If the leading-module is turned-off, the iLLC resonant converter will degrade to be a traditional full-bridge LLC resonant converter operating at its resonant frequency. The equivalent circuit and key waveforms of this situation are shown in Fig. 8. In this case, the operation principles are the same as the conventional LLC resonant converter. The
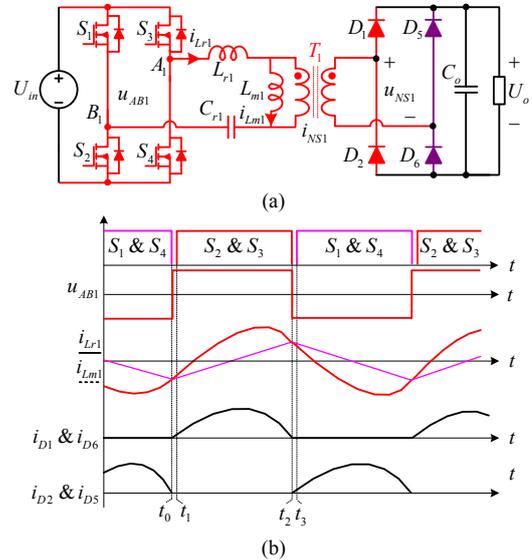

Fig. 8. Equivalent circuit and key waveforms when φ=0 and the leading-module is turned-off, (a) equivalent circuit, (b) key waveforms.

detailed operation will not be analyzed here.

IV. CHARACTERISTICS AND ANALYSIS

A. Voltage Gain

1) Variable-Frequency Mode

When the iLLC resonant converter operates in the

variable-frequency mode, the voltage gain characteristic is the same as the conventional LLC resonant converter. Since the primary-side of the two LLC modules are in-parallel while the secondary windings are in-series, the voltage gain of the iLLC resonant converter is two times of each LLC module, i.e. $G_i=2G_{LLC}$. For simplicity, it is assumed that $L_{r1}=L_{r2}=L_r$, $L_{m1}=L_{m2}=L_m$. Using the fundamental harmonic analysis (FHA) method [12], the voltage gain in the variable-frequency mode can be expressed as:

$$G_i = \frac{U_o}{NU_{in}} = 2G_{LLC} = \frac{2}{\sqrt{[1+\frac{1}{k}(1-\frac{1}{f_N^2})]^2 + Q_r^2(f_N - \frac{1}{f_N})^2}} \quad (4)$$

where

$$k = \frac{L_m}{L_r}, \quad f_N = \frac{f_S}{f_r} \quad (5)$$

$$f_r = \frac{1}{2\pi\sqrt{L_r C_r}} \quad (6)$$

$$Q_r = \frac{2N^2 Z_r}{R_o} \quad (7)$$

$$Z_r = \sqrt{\frac{L_r}{C_r}} \quad (8)$$

and R_o is the load resistance of the iLLC converter. It should be noted that the maximum switching frequency of the iLLC resonant converter is f_r, which means the iLLC will not enter the $f_S > f_r$ region, in which the rectifying diodes are hard-switched.

2) Fixed-Frequency Phase-Shift Mode

When the iLLC converter works in the phase-shift mode, the switching frequency is fixed at f_r. It is obvious that the normalized voltage gain $G_i=2$ if the phase shift angle $\varphi=\pi$, while $G_i=1$ if $\varphi=0$. Therefore, it is easy to understand that the output voltage is proportional to the phase shift angle φ, and the normalized voltage gain can be continuously regulated between 1 and 2 by varying φ between 0 and π. However, when the converter operates in the phase-shift mode, it is difficult to obtain a numerical solution for the voltage gain G_i because the multiple resonant stages will lead to a transcendental equation. In order to simplify the analysis and derive the relation between G_i and φ, the magnetizing inductance of the two transformers T_1 and T_2 are ignored in the following analysis.

In order to fully understand the voltage gain characteristic of the proposed iLLC resonant converter in the phase shift mode, the steady-state trajectory curve of the resonant network composed of L_{r1} and C_{r1} is shown in Fig. 9, where the inductor current is multiplied by the impedance Z_r of the resonant tank. Seen from the trajectory curve, the Stage I and Stage II in the phase shift mode can be simplified to the Stage A in Fig. 9. During the Stage A, U_{in} supplies power to the load through both the two transformers T_1 and T_2, the secondary windings of T_1 and T_2 are connected in series, and the converter moves along the trajectory curve from point A_1 to A_2. The center point O_1 around which the L_{r1} and C_{r1} resonate is located at ($U_{in} - \frac{U_o}{2N}$, 0), and the i_{Lr1} and u_{Cr1} are
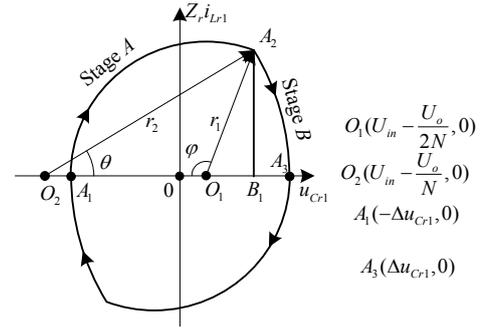

Fig. 9. Trajectory curve of state variables in the iLLC resonant converter.

expressed as follows.

$$i_{Lr1}(t) = \frac{r_1}{Z_r}\sin[\omega_r(t-t_0)] \quad (9)$$

$$u_{Cr1}(t) = (U_{in} - \frac{U_o}{2N}) - r_1\cos[\omega_r(t-t_0)] \quad (10)$$

where $\omega_r = 2\pi f_r$ and the radius r_1 of the trajectory curve

$$r_1 = U_{in} - \frac{U_o}{2N} + \Delta u_{Cr1} \quad (11)$$

$$\Delta u_{Cr1} = \frac{P_1}{4U_{in}f_s C_r} \quad (12)$$

P_1 is the average output power transferred by the transformer T_1.

When the switches S_6 & S_7 are turned OFF at t_2, the converter enters the resonant Stage B in Fig. 9, during which only the transformer T_1 supplies power to the load. In the Stage B, the converter moves along the trajectory curve from point A_2 to A_3. The center point O_2 around which the L_{r1} and C_{r1} resonate is located at ($U_{in} - \frac{U_o}{N}$, 0), and the i_{Lr1} and u_{Cr1} are expressed as follows.

$$i_{Lr1}(t) = \frac{r_2}{Z_r}\sin[\theta - \omega_r(t-t_2)] \quad (13)$$

$$u_{Cr1}(t) = (U_{in} - \frac{U_o}{N}) + r_2\cos[\theta - \omega_r(t-t_2)] \quad (14)$$

The radius r_2 of the trajectory curve

$$r_2 = \frac{U_o}{N} - U_{in} + \Delta u_{Cr1} \quad (15)$$

According to (9)-(15), the following equation is satisfied at t_2:

$$i_{Lr1}(t_2) = \frac{r_1}{Z_r}\sin\varphi = \frac{r_2}{Z_r}\sin\theta \quad (16)$$

Therefore the phase shift angle θ is derived as:

$$\theta = \arcsin(\frac{r_1}{r_2}\sin\varphi) \quad (17)$$

According to the operation principles of the iLLC resonant converter in the phase shift mode, the leading LLC module only transfers power to the load during the resonant Stage A, while the lagging LLC module transfers power to the load during the resonant Stage A and B. Therefore, the average output power transferred by the transformer T_1 is
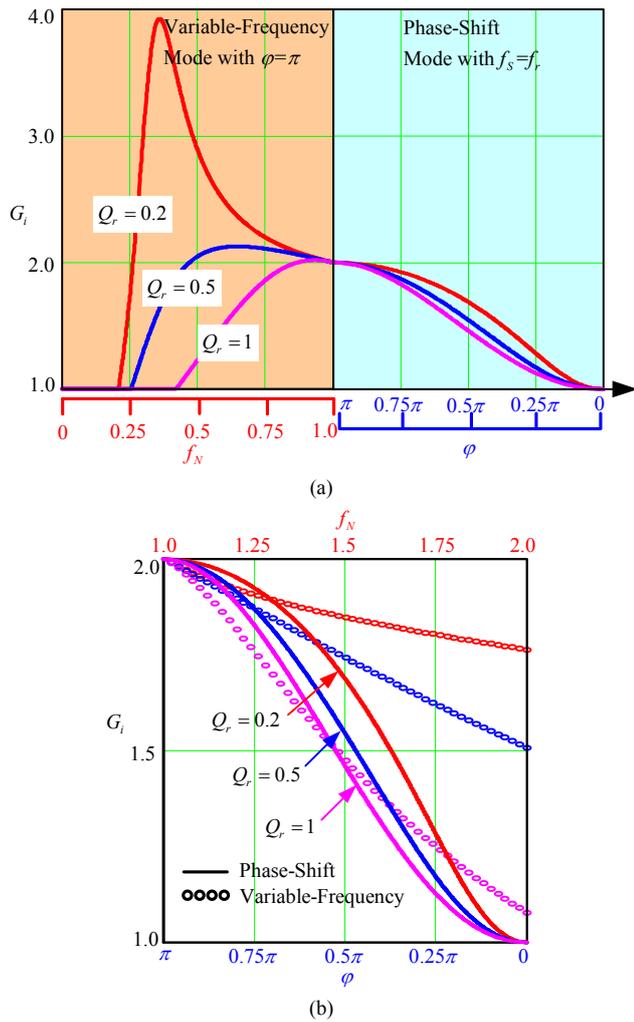
Fig. 10. Voltage gain curves, (a) voltage gain of the proposed iLLC converter, (b) comparison between phase-shift control and variable frequency control.

$$P_1 = U_o \frac{\int_0^{t_S} i_{Lr1}(t)dt}{NT_S/2} \qquad (18)$$

In the resonant Stage A, the secondary-windings of the two transformers are connected in series and transfer power to the load simultaneously. Therefore, if the magnetizing current of the two transformers is ignored for simplicity, the resonant current of the two modules should be the same, i.e. $i_{Lr1}=i_{Lr2}$, even though the voltages of the two resonant capacitors are not the same. Therefore, the average output power transferred by the transformer T_2 is calculated as follows:

$$P_2 = U_o \frac{\int_0^{t_2} i_{Lr1}(t)dt}{NT_S/2} \qquad (19)$$

Ignoring the power conversion losses, the output power can be calculated as:

$$P_o = P_1 + P_2 = \frac{U_o^2}{R_o} \qquad (20)$$

where R_o is the load resistance. Substituting (1) and (9)-(19) into (20), the following equation is derived

$$\pi Q_r[2 - (\sin\frac{\varphi}{2})^2]G_i^3 + [6(\sin\frac{\varphi}{2})^2 - 2\pi Q_r]G_i^2$$
$$-16(\sin\frac{\varphi}{2})^2 G_i + 8(\sin\frac{\varphi}{2})^2 = 0 \qquad (21)$$

According to (21), the relationship between the normalized voltage gain G_i and the phase shift angle φ is given by

$$\varphi = \arcsin(G_i\sqrt{\frac{2\pi Q_r(G_i-1)}{\pi Q_r G_i^3 - 6G_i^2 + 16G_i - 8}}) \qquad (22)$$

Based on (4) and (22), the voltage gain curves of the proposed iLLC resonant converter are shown in Fig. 10. The curves of variable frequency control are plotted with k=8. Fig. 10(a) is the voltage gain curves of the iLLC resonant converter with the variable-frequency plus phase-shift control. It can be seen that the output voltage can be regulated in a wide range with a very narrow switching frequency range. G_i=2 when f_S=f_r and φ=π. The converter operations in the variable-frequency mode and the switching frequency f_S<f_r when G_i>2, whereas f_S stays at f_r and the converter operates in the phase-shift mode when G_i<2. The comparison between the phase-shift control and the traditional variable frequency control is illustrated in Fig. 10(b). It is seen that the normalized voltage gain drops slowly in the f_S>f_r region. For example, G_i only decreases to 1.7 when Q_r=0.2 and f_S has increased to two times of the resonant frequency f_r. It means a much higher switching frequency is needed to obtain the same output voltage range if only variable frequency control is employed. In addition, it can be seen that the voltage regulation of phase-shift control is not sensitive to the output load, i.e. the quality factor Q_r, whereas the variable frequency is very sensitive to Q_r. That's why the conventional LLC resonant converter is difficult to control under light load condition.

B. Soft-Switching Performance

According to the operation principles, it is seen that zero-voltage turn-ON and zero-current OFF can be achieved for all the active switches and rectifying diodes in both variable-frequency and phase-shift modes. Therefore, excellent soft-switching performance within the entire operation range can be achieved with the proposed iLLC resonant converter as well, which is the same as the conventional LLC resonant converter. Meanwhile, another advantage of the proposed iLLC resonant converter in comparison with the traditional LLC resonant converter is that the switching frequency range of the resonant tank is reduced. Therefore, the output voltage can be regulated in a wide range without varying the switching frequency in a wide range. Meanwhile, since the operation range of the variable-frequency mode is narrowed, the circulating current and the additional conduction losses associated with the magnetizing inductance can be reduced as well.

C. Circulating Current Analysis

The advantage of excellent soft-switching performance of traditional LLC resonant converter has been maintained by the proposed iLLC converter. However, it should be noted that, the iLLC converter still has some drawbacks when it operates in the phase-shift mode. According to the operation
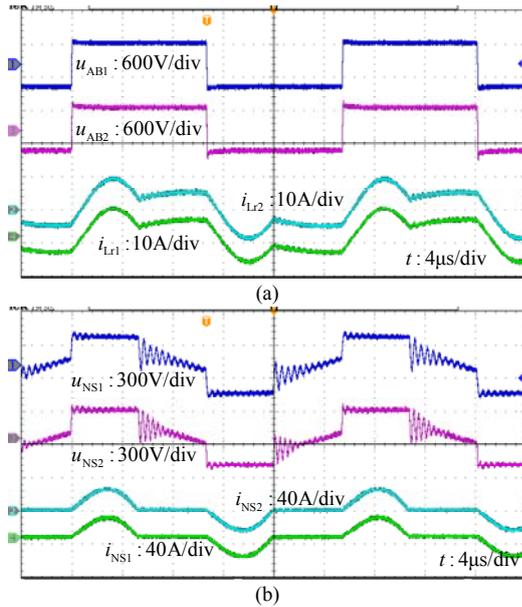
Fig. 11. Switching waveforms at U_o=500V, (a) u_{AB1}, u_{AB2}, i_{Lr1} and i_{Lr2}, (b) u_{NS1}, u_{NS2}, i_{NS1} and i_{NS2}.

principles in the phase-shift mode, in the Stage III and Stage IV of the phase-shift mode, the secondary winding of T_2 is shorted and the current i_{Lr2} is recycled to the input instead of transferred to the output. Therefore, the current of i_{Lr2} in the Stage III and Stage IV represents a circulating current, which will lead to additional conduction loss. According to the waveform of resonant current i_{Lr2}, the circulating current increases as the phase shift angle φ approaches to $\pi/2$, and decreases when φ approaches to 0 or π. Hence, it can be estimated that, when the iLLC operates in the phase shift mode, the conversion efficiency decreases when the phase shift angle φ increases from 0 to $\pi/2$, and the efficiency would increase when the phase shift angle φ increases from $\pi/2$ to π.

V. EXPERIMENTAL EVALUATION AND ANALYSIS

A 3.5kW experimental prototype is built based on the proposed full-bridge iLLC resonant converter to evaluate the performance of the proposed iLLC resonant converter and its control strategies. The input voltage U_{in}=400V±10V, output voltage U_o=150V-500V, the maximum output current I_{omax}=7A. To fully utilize the output voltage regulation capability of the phase-shift mode, the turns ratio of the two transformers is designed to be N=3:8, in which case the output voltage range of the variable frequency mode is 300V-500V while the output voltage range of the fixed-frequency phase-shift mode is 150V-300V. The output voltage U_o=300V when f_S=f_r and φ=π is 300V, and U_o=150V when φ=0. The resonant frequency f_r of the resonant tank in the iLLC converter is 100kHz. The devices' parameters in the prototype are as follows. L_{r1}=53.8uH, L_{r2}=53.9uH, C_{r1}=C_{r2}=47nF, L_{m1}=L_{m2}=430uH, S_1-S_8: IXFH22N60P, D_1-D_6: DSEK60-06A.

The steady-state experimental waveforms when U_o=500V are shown in Fig. 11. Fig. 11(a) is the waveforms of the primary side voltages u_{AB1}, u_{AB2} and currents i_{Lr1} and i_{Lr2}, whereas Fig. 11(b) is the waveforms of the secondary side
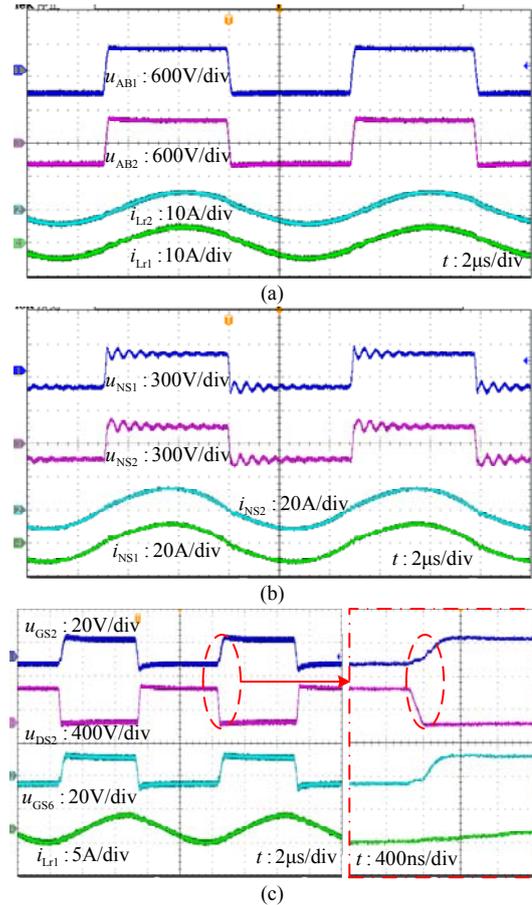

Fig. 12. Switching waveforms at U_o=300V, (a) u_{AB1}, u_{AB2}, i_{Lr1} and i_{Lr2}, (b) u_{NS1}, u_{NS2}, i_{NS1} and i_{NS2}, (c) u_{GS2}, u_{DS2}, u_{GS6} and i_{Lr1}.

voltages u_{NS1}, u_{NS2} and currents i_{NS1} and i_{NS2}. When the output voltage U_o is 500V, the iLLC resonant converter operates in the variable frequency mode with f_S<f_r. It is seen that the waveforms of i_{Lr1} and i_{Lr2} are the same as that in a traditional variable-frequency modulated LLC resonant converter. Meanwhile, since the phase-shift angle φ is kept at its maximum value, i.e. φ=π, the two secondary windings of the two transformers are always connected in series. Therefore, as shown in the experimental waveforms, the voltages u_{AB1} and u_{AB2}, and the voltages u_{NS1} and u_{NS2} are always in phase. The currents i_{Lr1} and i_{Lr2} are equal, while i_{NS1} and i_{NS2} are equal, which means the output power is shared equally by the two LLC modules and two transformers.

The steady-state waveforms when U_o=300V are shown in Fig. 12, where the iLLC resonant converter works in the boundary of variable-frequency mode and phase-shift mode with f_S=f_r and φ=π. Fig. 12(a) is the waveforms of primary-side voltages u_{AB1}, u_{AB2} and currents i_{Lr1}, i_{Lr2}, Fig. 12(b) is the waveforms of secondary-side voltages u_{NS1}, u_{NS2} and currents i_{NS1}, i_{NS2}. Fig. 12(c) is the soft-switching waveforms of the primary-side switch S_2. It is seen that the switching frequency equals to the resonant frequency. u_{AB1}, i_{Lr1}, u_{NS1} and i_{NS1} are in phase with u_{AB2}, i_{Lr2}, u_{NS2} and i_{NS2}, respectively, which indicates that the two secondary-windings of the two transformers T_1 and T_2 work in series and the output power is shared equally by the two LLC modules. The waveforms shown in Fig. 12(c) indicate that soft-switching of
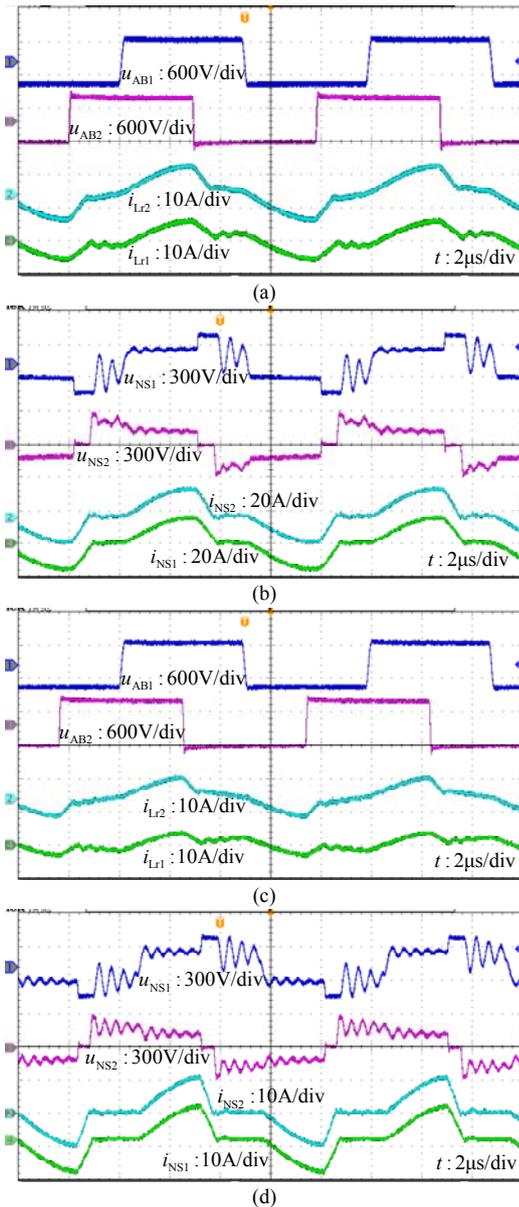
Fig. 13. Switching waveforms at U_o=250V, (a) u_{AB1}, u_{AB2}, i_{Lr1} and i_{Lr2} at full-load, (b) u_{NS1}, u_{NS2}, i_{NS1} and i_{NS2} at full-load, (c) u_{AB1}, u_{AB2}, i_{Lr1} and i_{Lr2} at half-load, (d) u_{NS1}, u_{NS2}, i_{NS1} and i_{NS2} at half-load.

Fig. 14. Soft-switching waveforms at the phase-shift mode, (a) u_{GS2}, u_{DS2}, u_{GS6} and i_{Lr1}, (b) u_{GS2}, u_{GS6}, u_{DS6} and i_{Lr2}.

Fig. 15. ZCS waveforms of the rectifying diode in the leading-module, (a) variable-frequency mode, (b) fixed frequency mode.

the primary side switch is achieved.

The steady-state waveforms when U_o=250V are shown in Fig. 13, where the iLLC resonant converter works in the fixed-frequency phase-shift mode. Fig. 13(a) and (b) are tested at full-load condition while Fig. 13(c) and (d) are tested at half-load condition. It is seen that the voltage u_{AB1} produced by the switches S_1-S_4 lags the voltage u_{AB2} produced by the switches S_5-S_8. From the current waveforms of i_{Lr1}, i_{Lr2}, i_{NS1} and i_{NS2}, it can be seen that the resonant inductors L_{r1} and L_{r2} begin to resonate with the capacitors C_{r1} and C_{r2} when the lagging voltage u_{AB1} commutates. When the two secondary windings works in in-series mode, the current i_{NS1} and i_{NS2} are the same, which means the two transformers supply power to the load simultaneously. When the leading voltage u_{AB2} commutates, the voltage u_{NS2} is zero in a short interval, which means the secondary winding of T_2 is shorted by the hybrid
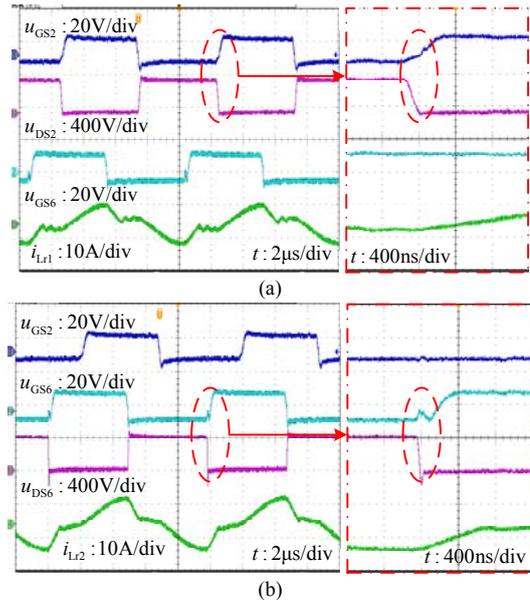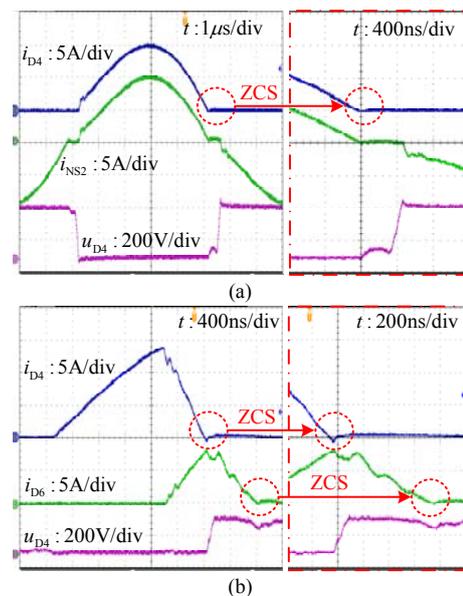
rectifier. It should be noted that the voltage rings on the secondary winding u_{NS1} and u_{NS2} are induced by the resonance between the leakage inductance of transformers and the parasitic capacitance of the diodes D_5 and D_6 in the hybrid rectifier. In addition to the voltage rings of u_{NS1} and u_{NS2}, the experimental waveforms coincide with the theoretical analysis pretty well. Meanwhile, it is seen that the waveforms with half-load are similar to the waveforms with full-load, and the phase-shift angle under half-load is slightly lower than that under full-load, which indicates that the phase shift angle is proportional to the output load but not sensitive to the output load. This feature can be observed from the voltage gain curves shown in Fig. 10 as well.

When the converter operates in the phase-shift mode, the zero voltage switching waveforms of the switch S_2 in the
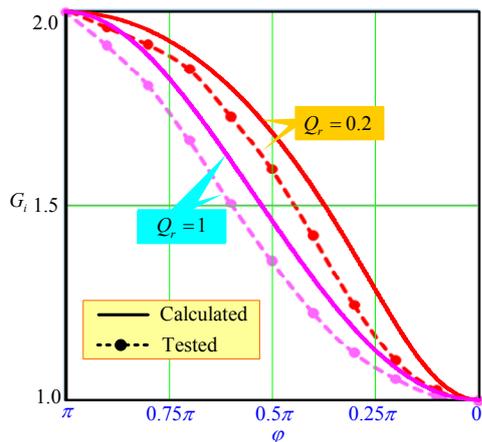
Fig. 16. Voltage gain curves of the iLLC converter in the fixed-frequency mode.
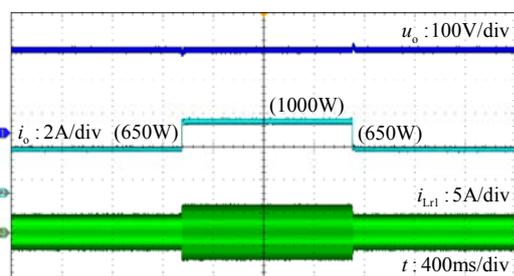

Fig. 17. Experimental waveforms with load step-up/down in the phase shift mode.

lagging-module and the switch S_6 in the leading-module are shown Fig. 14(a) and (b), respectively. It is seen that zero voltage switching has been achieved for both the switches in the leading-module and lagging-module. Since the switches S_1-S_4 operate in a symmetrical manner, so do switches S_5-S_8. It is proven that zero voltage switching is achieved for all the primary side switches.

The zero-current switching (ZCS) waveforms of the rectifying diodes in the leading-module are tested and shown in Fig. 15, where Fig. 15(a) is tested in the variable-frequency mode with $f_s<f_r$, while Fig. 15(b) are tested in the fixed-frequency mode. It is seen that ZCS of the rectifying diodes, D_4 and D_6, have been achieved in the fixed-frequency mode. However, the ZCS waveforms in the fixed-frequency mode are not as good as that in the variable-frequency mode. It is because the current slew rate in the fixed frequency mode is faster than that in the variable-frequency mode when the diodes' current decrease to zero. Therefore, a very slight reverse current is observed from Fig. 15(b). However, since the current slew rate is always limited by the resonant inductor, the reverse current and its related loss is very low.

The voltage gain curves of the proposed iLL resonant converter in the fixed-frequency mode are tested and compared with the theoretical analysis, as shown in Fig. 16. It is seen that the trend of the tested voltage gain curves coincides with the theoretical analysis very well. However, the tested voltage gain is lower than the calculated results. The main reason is that the real quality factor Q_r is greater than the theoretical one. In theoretical analysis, the load resistance is directly reflected to the primary side and used to
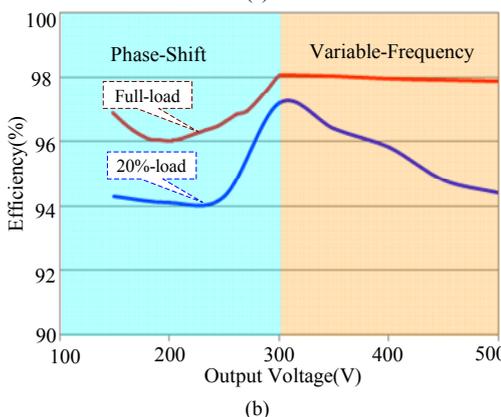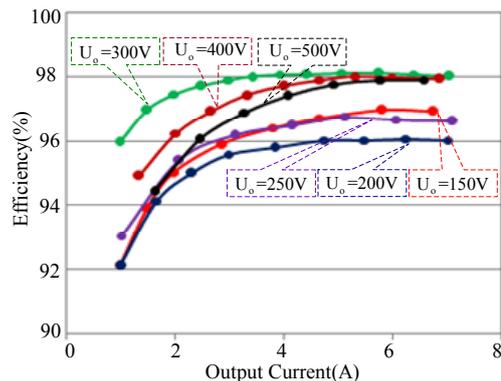

(a)

(b)

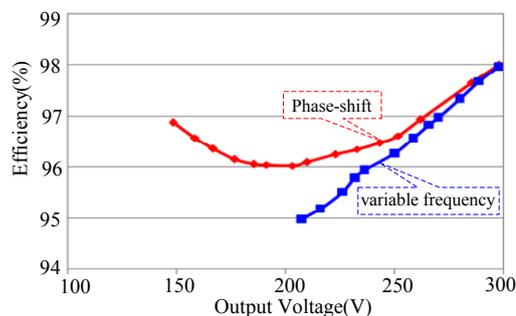Fig. 18. Efficiency curves, (a) efficiency versus output current, (b) efficiency versus output voltage.

Fig. 19. Efficiency comparison.

calculate the quality factor Q_r. But the real equivalent load resistance reflected to the resonant tank is lower than the load resistance.

The dynamic waveforms with load step-up and step-down in the phase-shift mode are shown in Fig. 17. It can be seen that the output voltage is stable when load steps-up/down, which indicates a good output voltage regulation performance of the phase-shift control.

The efficiency curves of the proposed full-bridge iLLC resonant converter are shown in Fig. 18. The curves in Fig. 18(a) are tested under different output current. It is seen that efficiency greater than 96% has been achieved in a wide load range when output voltage varies from 500V to 150V, the highest efficiency is up to 98%, and the best efficiency curve is obtained when U_o=300V with $f_S=f_r$ and $\varphi=\pi$. It is because that both the switching losses and conduction losses are minimized at the boundary of variable-frequency and

phase-shift modes. The efficiency curves with respect to output voltage are shown in Fig. 18(b). It is seen that a very flat efficiency curve is achieved when the converter works with full load and in the variable-frequency mode. It is because a wide output voltage range is covered by the phase-shift mode, and the output voltage regulation range is narrowed. Therefore, the conduction losses associated with the magnetizing inductance of transformers are reduced. However, the influence of the circulating current associated with the magnetizing inductance is very clear when the converter works at light load condition. As shown in Fig. 18(b), the efficiency curve at 20% load in the variable frequency mode drops rapidly when the output voltage increases.

The efficiency curves shown in Fig. 18(b) indicate that with the decreasing of output voltage, the trend of efficiency curves in the phase-shift mode is first falling then rising. As analyzed above, the current of i_{Lr2} in the Stage III and Stage IV of the phase-shift mode represents a circulating current, which will lead to additional conduction loss. The circulating current increases as the phase shift angle φ approaches to $\pi/2$, and decreases when φ approaches to 0 or π. Therefore, the circulating current reach its maximum value when $\varphi=\pi/2$. As a result, the conduction loss and turned-OFF loss of the switches in the leading-module reach their maximum values when $\varphi=\pi/2$ as well. That's why the trend of efficiency curves in the phase-shift mode is first falling then rising. From the efficiency curves, it is seen that the efficiency in the phase-shift mode is lower than that in the variable-frequency mode. However, if the output voltage range of variable-frequency mode is extended, the overall efficiency of the variable-frequency mode will decrease as well. For example, in comparison with the variable-frequency controlled improved LLC resonant converters in [18]-[20], the conversion efficiency of the proposed iLLC resonant converter is still higher, even when the converter operates in the fixed-frequency mode. In practice, the operation voltage range and the conversion efficiency of the variable-frequency mode are contradictory. A trade-off between the operation voltage range and the overall conversion efficiency must be made for the variable-frequency mode. Nevertheless, the proposed iLLC resonant converter and the phase-shift control provide a new control freedom for the traditional LLC resonant converter. The output voltage range of the variable frequency mode can be narrowed significantly by introducing the phase shift control.

The main objective of this research is providing a new voltage regulation method and extending the voltage gain range of the LLC resonant converter without pushing the switching frequency into the $f_s>f_r$ region. Fig. 19 shows the efficiency comparison results between the proposed control method and the variable-frequency control at full-load condition. For the variable-frequency control, the current is always shared by the two modules, but the switching frequency must be higher than f_r when the output voltage is lower than 300V. It is obvious that the lower the output voltage is, the more obvious the advantage of the proposed fixed-frequency control is. In our test, the switching frequency has been up to 2.5 times of f_r when the output voltage is 200V. Therefore, the efficiency of

variable-frequency control with output voltage lower than 200V is not tested any more.

VI. CONCLUSION

Interleaved LLC resonant converters with hybrid rectifier and variable-frequency plus phase-shift control are proposed for wide output voltage range applications. Theoretical analysis and experimental results indicate that a new control freedom is provided and the output voltage can be regulated in a wide range by employing phase-shifting control between the two interleaved LLC modules. The connection of the transformers' secondary-windings of the two LLC modules can be regulated with help of the hybrid rectifier and fixed-frequency phase-shift control. In addition, zero voltage switching of primary-side switches and zero current switching of secondary side rectifying diodes can be always achieved. The advantages of variable frequency control and phase-shift control are combined. Therefore, in comparison with the traditional variable-frequency controlled LLC resonant converter, the switching frequency range of the proposed interleaved LLC resonant converter is narrowed significantly. Hence, the circulating current and additional conduction losses associated with the magnetizing inductance of the LLC resonant converter is reduced dramatically. As a result, the contradiction between efficiency and voltage range of LLC resonant converters is solved. Effectiveness and feasibility of the proposed solution has been evaluated and verified by experimental results on a 3.5kW prototype with 400V input voltage and 150V-500V output voltage.

REFERENCES

[1] Z. Hu, Y. Qiu, L. Wang, Y.-F. Liu, "An interleaved LLC resonant converter operating at constant switching frequency," IEEE Trans. Power Electronics, vol. 29, no. 6, pp. 2931-2943.

[2] I. Demirel, B. Erkmen, "A very low-profile dual output LLC resonant converter for LCD/LED TV applications," IEEE Trans. Power Electronics, vol. 29, no. 7, pp. 3514-3524, July 2014.

[3] M. A. Saket, N. Shafiei, M. Ordonez, M. Craciun, C. Botting, "Low parasitics planar transformer for LLC resonant battery chargers," IEEE APEC, 2016, pp. 854-858.

[4] G. Yang, P. Dubus, D. Sadarnac, "Double-phase high-efficiency, wide load range high-voltage/ low-voltage LLC DC/DC converter for electric/hybrid vehicles," IEEE Trans. Power Electronics, vol. 30, no. 4, pp. 1876-1886, Apr. 2015.

[5] X. Sun, Y. Shen, Y. Zhu, X. Guo, "Interleaved boost-integrated LLC resonant converter with fixed-frequency PWM control for renewable energy generation applications," IEEE Trans. Power Electronics, vol. 30, no. 8, pp. 4312-4326, Aug. 2015.

[6] C.-H. Chang, C.-A. Cheng, H.-L. Cheng, "Modeling and design of the LLC resonant converter used as a solar-array simulator," IEEE Journal of Emerging and Selected Topics in Power Electronics, vol. 2, no. 4, pp. 833-841, Dec. 2014.

[7] H. Wang, Y. Chen, Y.-F. Liu, J. Afsharian, Z. Yang, "A new LLC converter family with synchronous rectifier to increase voltage gain for hold-up applications," IEEE ECCE, 2015, pp. 5447-5453.

[8] Z. Hu, L. Wang, H. Wang, Y.-F. Liu, P. C. Sen, "An accurate design algorithm for LLC resonant converters-part I," IEEE Trans. Power Electronics, vol. 31, no. 8, pp. 5435-5447, Aug. 2016.

[9] F. Musavi, M. Craciun, D. S. Gautam, W. Eberle, W. G. Dunford, "An LLC resonant DC-DC converter for wide output voltage range battery charging applications," IEEE Trans. Power Electronics, vol. 28, no. 12, pp. 5437-5445, Dec. 2013.

[10] Z. Fang, T. Cai, S. Duan, C. Chen, "Optimal design methodology for LLC resonant converter in battery charging applications based on

time-weighted average efficiency," IEEE Trans. Power Electronics, vol. 30, no. 10, pp. 5469-5483, Oct. 2015.

[11] R. Yu, G. K. Y. Ho, B. M. H. Pong, B. W.-K. Ling, J. Lam, "Computer-aided design and optimization of high-efficiency LLC series resonant converter," IEEE Trans. Power Electronics, vol. 27, no. 7, pp. 3243-3456, July 2012.

[12] R. Beiranvand, B. Rashidian, M. R. Zolghadri, S. M. H. Alavi, "A design procedure for optimizing the LLC resonant converter as a wide output range voltage source," IEEE Trans. Power Electronics, vol. 27, no. 8, pp. 3749-3763, Aug. 2012.

[13] W. Feng, F. C. Lee, P. Mattavelli, "Optimal trajectory control of burst mode for LLC resonant converter," IEEE Trans. Power Electronics, vol. 28, no. 1, pp. 457-466, Jan. 2013.

[14] S. Zhao, J. Xu, O. Trescases, "Burst-mode resonant LLC converter for an LED luminaire with integrated visible light communication for smart buildings," IEEE Trans. Power Electronics, vol. 29, no. 8, pp. 4392-4402, Aug. 2014.

[15] N. Shafiei, M. Ordonez, M. Craciun, C. Botting, M. Edington, "Burst mode elimination in high-power LLC resonant battery charger for electric vehicles," IEEE Trans. Power Electronics, vol. 31, no. 2, pp. 1173-1188, Feb. 2016.

[16] J.-H. Kim, C.-E. Kim, J.-K. Kim, J.-B. Lee, G.-W. Moon, "Analysis on load-adaptive phase-shift control for high efficiency full-bridge LLC resonant converter under light-load conditions," IEEE Trans. Power Electronics, vol. 31, no. 7, pp. 4942-4955, July 2016.

[17] H. Wu, T. Mu, X. Gao, Y. Xing, "A secondary-side phase-shift-controlled LLC resonant converter with reduced conduction loss at normal operation for hold-up time compensation application," IEEE Trans. Power Electronics, vol. 30, no. 10, pp. 5352-5357, Oct. 2015.

[18] Z. Liang, R. Guo, G. Wang, and A. Huang, "A new wide input range high efficiency photovoltaic inverter," in Proc. IEEE Energy Conversion Congr. and Expos., 2010, pp. 2937-2943.

[19] H. Hu, X. Fang, F. Chen, Z. J. Shen, and I. Batarseh, "A modified high-efficiency LLC converter with two transformers for wide input-voltage range applications," IEEE Trans. Power Electron., vol. 28, no. 4, pp. 1946-1960, Apr. 2013.

[20] H. Wu, Y. Li, Y Xing, "LLC resonant converter with semiactive variable-structure rectifier (SA-VSR) for wide output voltage range application," IEEE Trans. Power Electronics, vol. 31, no. 5, pp. 3389-3394, May 2016.

[21] P. Sun, L. Zhou, K. Ma, "A reconfigurable structure DC-DC converter with wide output range and constant peak power," IEEE Trans. Power Electronics, vol. 26, no. 10, pp. 2925-2935, Oct. 2011.

[22] X. Wu, H. Chen, J. Zhang, F. Peng, Z. Qian, "Interleaved phase-shift full-bridge converter with transformer winding series-parallel autoregulated (SPAR) current doubler rectifier," IEEE Trans. Power Electronics, vol. 30, no. 9, pp. 4864-4873, Sep. 2015.

[23] G. Zhang, X. Wu, W. Yuan, J. Zhang, Z. Qian, "A new interleaved active-clamp forward converter with parallel input and series-parallel output," IEEE APEC, 2009, pp. 40-44.

[24] X. Wu, H. Chen, " Two-phase hybrid forward convertor with series-parallel auto-regulated transformer windings and a common output inductor," Journal of Power Electronics, vol. 13, no. 5, pp. 757-765, 2013

[25] H. Chen, X. Wu, C. Hu, M. Chen, "A hybrid ZVS full-bridge converter with transformer winding series-parallel auto regulated current doubler rectifier," IEEE ECCE, 2012, pp. 2209-2214.
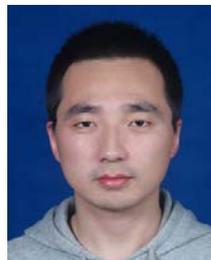
Hongfei Wu (S'11, M'13) was born in Hebei Province, China, in 1985. He received the B.S. and Ph. D degrees in electrical engineering and power electronics and power drives from Nanjing University of Aeronautics and Astronautics (NUAA), Nanjing, China, in 2008 and 2013, respectively. From June 2012 to July 2012, he was a gust PhD student at Institute of Energy Technology, Aalborg University, Denmark.

Since 2013, he has been with the Faculty of Electrical Engineering, NUAA, and is currently an Associate Professor with College of Automation Engineering, NUAA. He has authored and co-authored more than 100 peer-reviewed papers published in journals and conference proceedings. He is the holder of more than 20 Patents. His research interests are power converters, distributed power generation and spacecraft power system.

Dr. Wu was the recipient of the Outstanding Reviewer of *IEEE Transactions on Power Electronics* (2013).

Xiaohai Zhan was born in Hubei, China, in 1990.He received the B.S. degrees in electrical engineering and power electronics and power drives from Nanjing University of Aeronautics and Astronautics (NUAA), Nanjing, China, in 2014. He is currently working for the M.S. degree in electrical engineering from NUAA, Nanjing, China.

His research interests include topology and control of soft-switching dc-dc converters.

Yan Xing (M'03) was born in Shandong Province, China, in 1964. She received the B.S. and M.S. degrees in automation and electrical engineering from Tsinghua University, Beijing, China, in 1985 and 1988, respectively, and the Ph.D. degree in electrical engineering from Nanjing University of Aeronautics and Astronautics (NUAA), Nanjing, China, in 2000. Since 1988, she has been with the Faculty of Electrical Engineering, NUAA, and is currently a professor with College of Automation Engineering, NUAA. She has authored more than 100 technical papers published in journals and conference proceedings and has also published three books. Her research interests include topology and control for dc-dc and dc-ac converters.

Dr. Xing is an Associate Editor of the *IEEE Transactions on Power Electronics* and *Journal of Power Electronics*. She is a member of the Committee on Renewable Energy Systems within the IEEE Industrial Electronics Society.